

ORGANICCHEMISTRY

FRONTIERS







ORGANIC CHEMISTRY







FRONTIERS

RESEARCH ARTICLE



Cite this: *Org. Chem. Front.*, 2023, **10**, 5823

Repercussions of multi-electron uptake by a twistacene: a reduction-induced double dehydrogenative annulation†

Matthew Pennachio,^a Zheng Wei, ^b Robert G. Clevenger, ^b Kathleen V. Kilway, ^b Alexandra Tsybizova,^c Renana Gershoni-Poranne *d and Marina A. Petrukhina *d *a

Chemical reduction of highly-twisted 9,10,11,20,21,22-hexaphenyltetrabenzo[a,c,l,n]pentacene (C₇₄H₄₆, $\bf{1}$) was investigated using Li and Cs metals as the reducing agents. The Cs-induced reduction of $\bf{1}$ in the presence of 18-crown-6 ether enabled the isolation of a solvent-separated ion pair (SSIP) with a "naked" monoanion. Upon reduction with Li metal, a double reductive dehydrogenative annulation of $\bf{1}$ was observed to afford a new C₇₄H₄₂ $^{2-}$ dianion. The latter was shown to undergo a further reduction to C₇₄H₄₂ $^{4-}$ without additional core transformation. All products were characterized by single-crystal X-ray diffraction and spectroscopic methods. Subsequent in-depth theoretical analysis of one vs. two and four electron uptake by $\bf{1}$ provided insights into how the changes of geometry, aromaticity and charge facilitated the core transformation of twistacene observed upon two-fold reduction. These experimental and theoretical results pave the way to understanding of the reduction-induced core transformations of highly twisted and strained π -systems.

Received 12th August 2023, Accepted 17th September 2023 DOI: 10.1039/d3qo01282d

rsc.li/frontiers-organic

Introduction

Polycyclic aromatic hydrocarbons (PAHs) with non-planar, highly curved, or twisted frameworks are of great interest due to the effect such distortions have on their chemical, magnetic, electronic, optical, and chiroptical properties. Among the wide variety of known non-planar PAHs are the twistacenes – molecules of linearly annulated six-membered rings that bear bulky substituents and therefore typically adopt a helical (*i.e.*, "twisted") conformation to alleviate the resulting steric strain. Due to their non-planarity, twistacenes exhibit superior solubility and are very stable compared to their parent acenes, making them very attractive targets.

The injection of electrons into non-planar PAHs was shown to result in significant electronic and structural changes. $^{21-25}$ The studies of electron transfers of carbon bowls, 26 belts, 27 and wires 28 uncovered a prominent dependence on π -topology and charge. Remarkably, the chemical reduction of non-planar PAHs could lead to structural deformation, $^{28-41}$ new C–C bond formation, 42,43 and reductive dimerization. $^{44-47}$ For example, Scott and coworkers 48 found that the reduction of a 1,1′-binaphthyl moiety undergoes reductive cyclization to form perylene in the presence of potassium metal. Similarly, Ayalon and Rabinovitz 49 studied the dehydrogenative cyclization of [5]-helicene upon two-fold reduction with alkali metals. Recently, we demonstrated that strained mono- and bis-helicenes undergo reductive cyclization, driven by the relief of antiaromaticity. 50,51

Twistacenes provide a sterically crowded π -scaffold where dehydrogenation and C–C bond formation can also occur. ^{42,43} While there are some reports on the electrochemical behaviour of twistacenes, ^{20,52–62} the outcomes of chemical reduction of

Variation of the substituents allows one to tune the electronic properties of twistacenes, enabling their use in such diverse applications as light-driven molecular rotors, 10,11 stimuliresponsive molecular switches, 12 synthetic photovoltaic materials, 13,14 thermally activated delayed fluorescent materials, 15-17 nonlinear optical materials, 18 and light emitting diodes. 5,19,20

^aDepartment of Chemistry, University at Albany, State University of New York, Albany, NY 12222, USA. E-mail: mpetrukhina@albany.edu

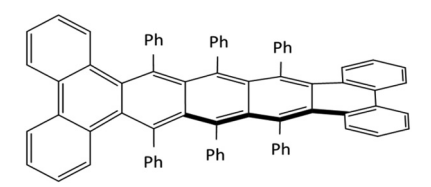
^bChemistry Discipline in the Division of Energy, Materials, and Systems, School of Science and Engineering, University of Missouri-Kansas City, Kansas City, MO 64110. USA

^cLaboratory for Organic Chemistry, ETH Zurich, Vladimir-Prelog-Weg 2, Zurich 8092, Switzerland

 $[^]d$ Schulich Faculty of Chemistry, Technion – Israel Institute of Technology, Technion City, Haifa 32000, Israel

[†] Electronic supplementary information (ESI) available: Details of preparation, X-ray diffraction and spectroscopic characterization, and computational studies. CCDC 2286322-2286324. For ESI and crystallographic data in CIF or other electronic format see DOI: https://doi.org/10.1039/d3qo01282d

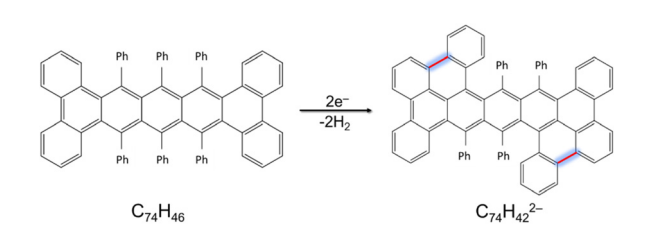
twistacenes have remained unexplored. To the best of our knowledge, no X-ray diffraction studies revealing structural consequences of electron addition to twistacenes or alkalimetal ion binding patterns to the twistacene anions have been reported. Herein, we carried out the first chemical reduction investigation of the twistacene 9,10,11,20,21,22-hexaphenyltetrabenzo[a,c,l,n] pentacene⁶³ (1, Scheme 1). This resulted in the isolation of several products in three different reduction states, which allowed us to reveal the reduction-induced core transformations. The products were fully characterized using single-crystal X-ray diffraction, NMR, EPR, and UV-Vis spectroscopy. In addition, a computational analysis was performed



Scheme 1 Twistacene 9,10,11,20,21,22-hexaphenyltetrabenzo[*a,c,l,n*] pentacene (1).

$$\begin{array}{c} \text{Cs, THF, 10 min} \\ \text{18-crown-6} \\ \text{1} \\ \text{10} \\ \text{Cs}^{+}_{2}(18-\text{crown-6})_{2}[1^{1-}]\cdot 2\text{THF (2}\cdot 2\text{THF)} \\ \text{18-crown-6} \\ \text{10} \\ \text{18-crown-6} \\ \text{18-crow$$

Scheme 2 Chemical reduction of 1 with Cs and Li in THF.



Scheme 3 Dehydrogenative annulation of twistacene **1** upon two-fold reduction.

to elucidate the electronic and structural responses to the addition of multiple electrons to 1.

Results and discussion

Chemical reduction of 1: crystallographic study of its monodoubly-, and tetra-reduced products

The chemical reduction of **1** with Cs and Li metals was investigated in THF at room temperature and monitored by UV-Vis absorption spectroscopy (Fig. S1 and S2†). The first reduction step is accompanied by the appearance of a deep purple colour. The reaction can be stopped at this stage and the resulting product stemming from the Cs-induced reduction was isolated using slow addition of hexanes into the THF reaction solution in the presence of 18-crown-6 ether. Single-crystal X-ray diffraction and EPR spectroscopic analysis (Fig. S13†) confirmed the formation of a solvent-separated ion pair of the mono-reduced anion with Cs⁺ counterion, namely $[Cs^+(18\text{-crown-6})_2][(1^{1-})]$ (crystallized with 2 interstitial THF molecules as 2-2THF, Scheme 2).

The use of an excess of lithium metal coupled with extended reaction time leads to a brown-black mixture indicating the formation of doubly-reduced anions in solution. Through slow addition of hexanes to the THF reaction solution, a new contact-ion product with lithium counterions was crystallized, as confirmed with single-crystal X-ray diffraction, namely [{Li⁺(THF₂)}₂(C₇₄H₄₂²⁻)] (crystallized with 3 interstitial THF molecules as 3.3THF, Scheme 2). Remarkably, the use of excess lithium and ultrasonication of the reaction mixture for one hour resulted in a highly-reduced product, isolated and identified single-crystal X-ray diffraction $[Li^{+}(THF)_{4}]_{2}[\{Li^{+}(THF)_{2}\}_{2}(C_{74}H_{42}^{4})]$ (crystallized with 0.5 interstitial THF molecules as 4.0.5THF, Scheme 2). Notably, upon addition of two electrons, the polycyclic aromatic core of 1 is transformed through two reductive C-C couplings to afford a new C₇₄H₄₂²⁻ dianion in 3 (Scheme 3). However, no further annulation is observed upon formation of a C74H424- tetraanion in 4 (vide infra).

The crystal structure of 2 consists of one Cs^+ ion sandwiched between two 18-crown-6 ether molecules ($Cs\cdots O_{crown}$, 3.2019(7)–3.559(2) Å)^{50,64} and one $C_{74}H_{46}^{1-}$ anion, forming a solvent-separated ion pair (Fig. 1). The isolation of this

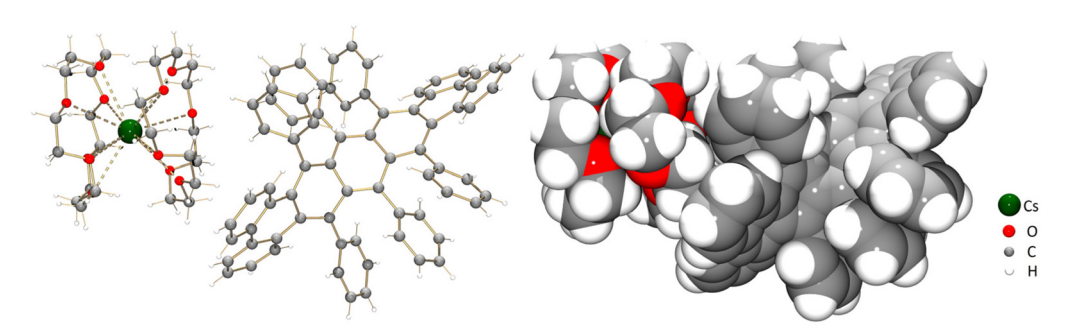


Fig. 1 Crystal structure of 2, ball-and-stick model (left) and space-filling model (right).

product allows structural analysis of the "naked" polycyclic twistacene core upon addition of one electron and without direct metal binding influence.

An X-ray diffraction study of 3 revealed that there are two crystallographically independent [Li⁺(THF)₂] cations bound to the $C_{74}H_{42}^{\ \ 2-}$ dianion core (Fig. 2). Since both cations show similar coordination environments, only one is discussed

Specifically, the [Li⁺(THF)₂] ion binds to four carbon atoms of the penultimate ring of the pentacene core of C₇₄H₄₂²⁻ (Li···C, 2.360(8)–2.575(8) Å) and to the *ipso*-carbon atom (Li···C, 2.408(9) Å). A longer contact to the adjacent carbon atom of 2.819(8) Å can be noted (Fig. 2c and Table S5†). Coordination of the Li⁺ ion is completed by two THF molecules with the Li···O_{THF} distances of 1.875(19) and 1.952(14) Å. All Li···C and Li···O distances are close to those previously reported.40,43

An X-ray diffraction study of 4 revealed that there are four crystallographically independent Li⁺ ions, with two [Li⁺(THF)₂] cations bound to the tetraanion and two [Li+(THF)4] cations remaining solvent-separated from the $C_{74}H_{42}^{4-}$ core (Fig. 3). As the coordination environment of two [Li⁺(THF)₂] cations is similar, only one is discussed in detail. Specifically, the Li⁺ ion with two coordinated THF molecules (Li...O_{THF}, 1.996(5) and 1.921(4) Å) binds to four carbon atoms of the penultimate ring of the pentacene core (Li···C, 2.360(8)-2.571(4) Å) and two carbons on the adjacent ring (Li···C, 2.415(9) and 2.714(4) Å) of $C_{74}H_{42}^{4-}$ (Table S5†). Notably, the Li⁺ ion binding sites of both anions, $C_{74}H_{42}^{2-}$ and $C_{74}H_{42}^{4-}$, in 3 and 4 are rather similar.

In the solid-state structure of 2, multiple C-H $\cdots\pi$ contacts (2.103(2)-2.787(3) Å) between the 1^{1-} anions and the $\{Cs^{+}(18-)\}$

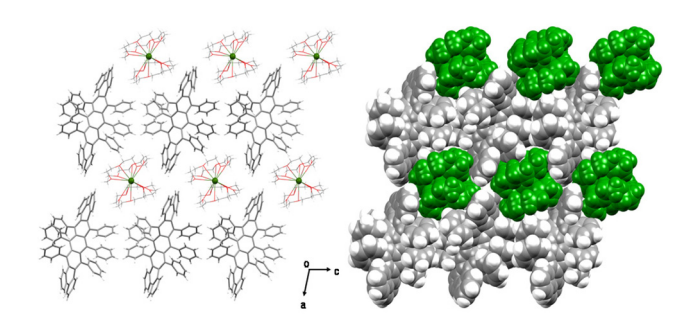


Fig. 4 Solid-state packing of 2, (left) mixed and (right) space-filling models. Interstitial THF molecules are removed. Cationic moieties are shown in green.

crown-6)₂} cations support the formation of a 2D network (Fig. 4 and Table S2†). In the solid-state structure of 3, two C- $H \cdots \pi$ contacts (2.200(14) Å) are found between the $C_{74}H_{42}^{2-}$ anions and the coordinated THF molecules of the adjacent moieties (Fig. 5 and S16†). The solid-state structure of 4 contains numerous C-H $\cdots\pi$ contacts (2.484(4)-2.791(5) Å) between the C₇₄H₄₂⁴⁻ anions and the coordinated THF molecules forming a 3D network (Fig. 6 and Table S3†).

Twistacene core deformation and transformation

The addition of one electron leads only to a slight structural deformation of the original twistacene framework, which can be illustrated by a direct comparison of C-C bond lengths between 1 and 11- (Table 1). For example, bonds d, h, k, and **m** are noticeably elongated ($\Delta_{avg.} = 0.020 \text{ Å}$), with **k** almost

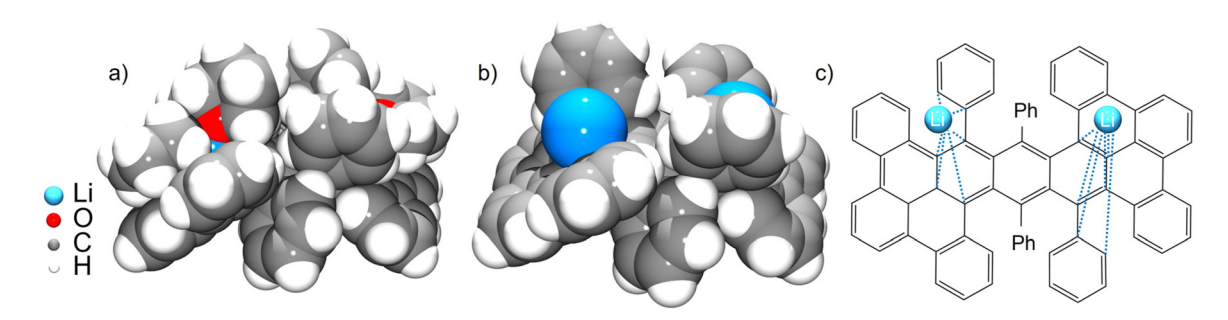


Fig. 2 Crystal structure of 3, space-filling model, with (a) and without coordinated THF (b), coordination of Li⁺ ions (c).

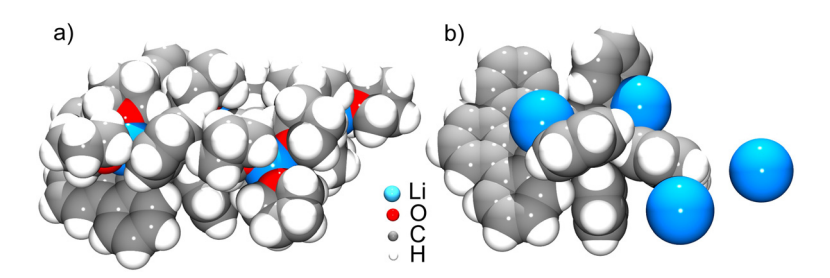


Fig. 3 Crystal structure of 4, space-filling model, with (a) and without coordinated THF (b).

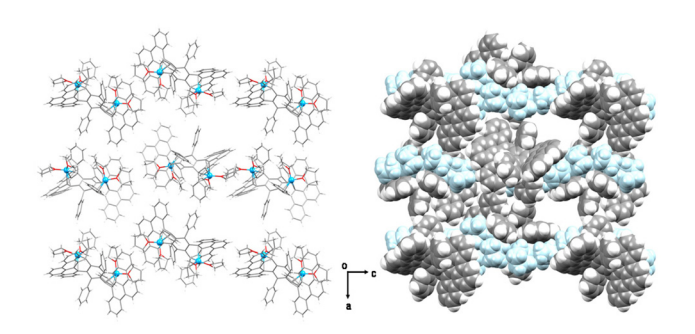


Fig. 5 Solid-state packing of 3, (left) mixed and (right) space-filling models. Interstitial THF molecules are removed. Cationic moieties are shown in blue

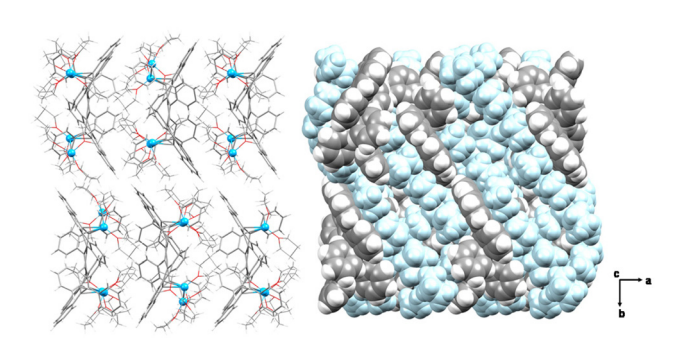


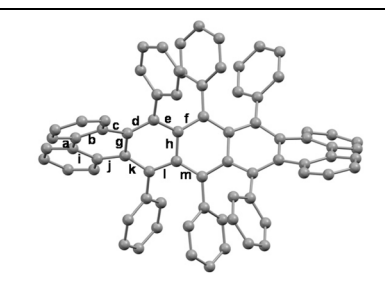
Fig. 6 Solid-state packing of **4**, (left) mixed and (right) space-filling models. Interstitial THF molecules are removed. Cationic moieties are shown in light blue.

0.03 Å longer than in the neutral parent. Conversely, bonds **c**, **g**, and **j** are slightly contracted by 0.011 Å, 0.012 Å, and 0.015 Å, respectively. In contrast to these bond alterations, the overall helical twist of the molecular skeleton is only modestly affected (Table S8†).

However, the addition of two electrons to twistacene results in more drastic changes, as the polycyclic aromatic core of 1 a two-fold dehydrogenative annulation accompanied by the formation of two new C-C bonds (Scheme 3). Notably, the molecular skeleton of the $C_{74}H_{42}^{2-}$ dianion is significantly altered compared to the neutral parent. 65,66 This can be illustrated by a direct comparison of C-C bond distances and torsional distortion between 1 and the $C_{74}H_{42}^{\ \ 2-}$ anion. The two newly formed C-C bonds, ${\bf r}$ and ${\bf s}$ (1.435(10) and 1.471(6) Å, respectively), expand the conjugated polycyclic core by inclusion of two more aromatic rings (Table 2). Bonds c, g, and o are noticeably shortened by 0.052, 0.056, and 0.039 Å, while bonds d, i, k, p, and l are elongated $(\Delta_{\text{avg.}} = 0.051 \text{ Å})$ with **k** elongated by almost 0.100 Å.

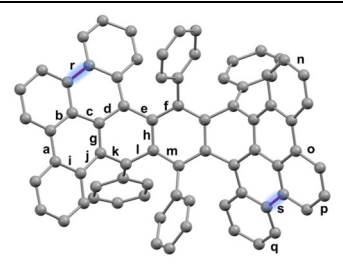
In 4, the polycyclic core of $C_{74}H_{42}^{\ 4-}$ retains the two-fold annulation observed in 3 (Scheme 3). The two corresponding C–C bonds, **r** and **s** measure at 1.456(2) and 1.451(3) Å, respectively. Comparison of the anionic carbon frameworks in 3 and 4 reveals their resemblance. Close examination of the C–C bond length distances of the central pentacene core in 3 and 4

Table 1 Key C-C bond distances (Å) in 1 and $\mathbf{1}^{1-}$, along with a labeling scheme



Bond	1	Cs- 1 ¹⁻
a	1.462(4)	1.4587(9)
b	1.410(5)	1.4181(8)
c	1.486(4)	1.4748(8)
d	1.386(4)	1.4076(8)
e	1.447(4)	1.4401(7)
f	1.421(4)	1.4198(8)
g	1.454(5)	1.4417(7)
ĥ	1.438(4)	1.4504(8)
i	1.416(4)	1.4204(8)
j	1.484(4)	1.4694(8)
k	1.380(5)	1.4084(7)
1	1.448(4)	1.4302(7)
m	1.416(4)	1.4335(7)

Table 2 Key C–C bond distances (Å) in **1**, $C_{74}H_{42}^{2-}$ in **3**, and $C_{74}H_{42}^{4-}$ in **4**, along with a labeling scheme



Bond	$C_{74}H_{46}$ 1	$\text{Li}_2\text{-C}_{74}\text{H}_{42}^{\ \ 2}$ 3	$\text{Li}_4\text{-C}_{74}{\text{H}_{42}}^{4-}4$
a	1.462(4)	1.455(11)	1.447(3)
b	1.410(5)	1.405(10)	1.435(2)
c	1.486(4)	1.434(10)	1.436(2)
d	1.386(4)	1.436(5)	1.435(2)
e	1.447(4)	1.469(5)	1.479(2)
f	1.421(4)	1.430(5)	1.429(2)
g	1.454(5)	1.398(5)	1.414(2)
h	1.438(4)	1.417(5)	1.422(2)
i	1.416(4)	1.432(10)	1.432(3)
j	1.484(4)	1.468(11)	1.428(2)
k	1.380(5)	1.476(5)	1.472(2)
1	1.448(4)	1.483(5)	1.484(2)
m	1.416(4)	1.414(5)	1.419(2)
n	1.386(4)	1.364(12)	1.404(3)
0	1.405(4)	1.366(9)	1.413(2)
р	1.385(4)	1.447(12)	1.380(3)
q	1.372(5)	1.337(12)	1.365(3)
r	()	1.435(10)	1.456(2)
S		1.471(6)	1.451(3)

illustrates that the majority are comparable, except for bonds **b** (elongated by 0.030 Å in **4**) and **j** (contracted by 0.040 Å in **4**). However, the C–C bonds on the peripheral phenyl rings reveal

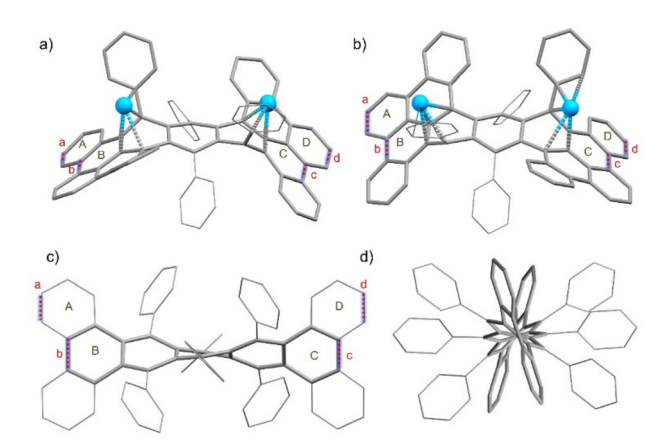


Fig. 7 Geometry of $C_{74}H_{42}^{2-}$ dianion (a) $C_{74}H_{42}^{4-}$ tetraanion (b), along with coordinated Li⁺ ions; geometry of neutral parent (c and d), mixed

more notable changes from $C_{74}H_{42}^{\ \ 2}$ to $C_{74}H_{42}^{\ \ 4}$, with bonds **n**, **o**, and **q** lengthened ($\Delta_{avg.} = 0.038 \text{ Å}$) and **p** shortened by 0.067 Å.

In addition to these bond alterations, the new C₇₄H₄₂²⁻ dianion and C₇₄H₄₂⁴⁻ tetraanion adopt the geometry of a positively curved PAH in contrast to the twisted nature of the neutral parent (Fig. 7 and Table S9†). The torsion angle of the central pentacene core (b/c) decreases from -143.36° in 1 to 12.30° (3) and -18.16° (4). In addition, the dihedral angle A-D increases from 41.35° in 1 to 71.83° (3) and 69.76° (4), further exemplifying the drastic geometry change. In both cases, the [Li⁺(THF)₂] moieties coordinate to the convex (exo) surface of the $C_{74}H_{42}^{2-}$ and the $C_{74}H_{42}^{4-}$ anions (Fig. 7).

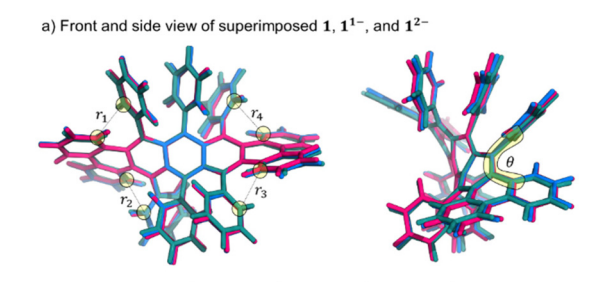
Computational investigation

The experimental evidence suggests that the mono-reduced twistacene, 11-, is relatively long-lived, whereas the doublyreduced 1²⁻ undergoes spontaneous double-cyclization upon formation. Additionally, the experimental evidence shows that the second core annulation proceeds regioselectively, as only one type of doubly-cyclized product is formed, with the two newly-formed rings on opposite sides of the pentacene moiety (i.e., trans). In other words, following the first cyclization event, there are three potential sites for the second cyclization, which could lead to different products (i.e., a cis-, gem-, or trans-type bis-cyclization). However, only the trans-type doublyannulated product is obtained, and the other theoretical possibilities are not observed. In order to gain a deeper understanding of the core transformation mechanism, including the origin of the regioselectivity, we performed a computational investigation focused on three aspects: (a) geometry, (b) frontier molecular orbitals, and (c) aromaticity.

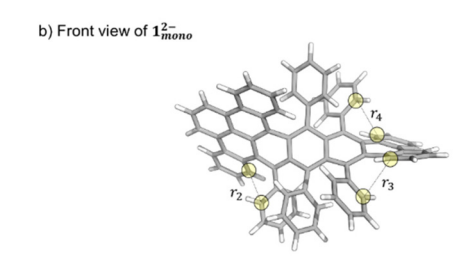
Geometry

To probe the geometrical features of the twistacene series, we fully optimized the structure of the naked neutral twistacene 1, as well as its reduced forms 1^{1-} and (undetected) 1^{2-} . It is noteworthy that the gas phase geometry optimization reduces the symmetry of the neutral molecule to C_1 and, as a result, there appear to be four non-identical potential sites for the first cyclization (depicted in Fig. 8A with highlighted circles and numbered 1-4). However, the ¹H NMR spectrum of 1 (Fig. S6 \dagger) shows only ten peaks, which is indicative of D_2 symmetry and points to a free rotation of the pendant phenyl groups in solution, thus making the four sites equivalent prior to the first cyclization. Nevertheless, the optimized geometry of 1 highlights the geometrical features at the minimumenergy conformer. We observe that the helical sites form two similar pairs, in which sites that are trans to one another are more similar than those that are *cis* or *gem*. The similarity was measured by the C-C distances between the carbon atoms that can bond through cyclization (denoted as r in Fig. 8a) and the dihedral angles of the helical sites (denoted as θ in Fig. 8a): r_1 = 3.122, r_2 = 3.184, r_3 = 3.135, r_4 = 3.162 Å and θ_1 = 16.17, θ_2 = 9.16, $\theta_3 = 17.35$, $\theta_4 = 8.40$. Specifically, the pair 1 and 3 have shorter C-C distances and larger dihedral angles than the pair 2 and 4.

The first reduction leads to a subtle shift in the twist of the pentacene core, which brings the pendant phenyl groups closer to the flanking rings. As a result, the distances rdecrease and the dihedral angles θ increase. As detailed in



Cmpd.	$ar{r}$ (Å)	θ (°)
1	3.151	12.772
11-	3.113	15.048
12-	3.070	17.183



r	r (Å)	θ (°)
2	3.130	22.819
3	3.007	13.044
3	3.131	21.897

Fig. 8 Comparison of structural changes between twistacene 1 (pink) and its reduced forms: 1^{1-} (blue), 1^{2-} (green), and 1_{mono}^{2-} (gray).

Fig. 8A, the average C–C distance for the four sites decreases from $\bar{r}=3.151$ Å to $\bar{r}=3.113$ Å. However, the shortening is not symmetric; r_1 and r_3 shorten more than r_2 and r_4 (average change is $\Delta \bar{r}=-0.047$ and -0.029 Å for the two pairs, respectively). The second reduction, to $\mathbf{1}^{2-}$, continues this trend. The C–C distances decrease to an average of $\bar{r}=3.070$ Å ($\Delta \bar{r}=-0.063$ Å for r_1 and r_3 and $\Delta \bar{r}=-0.022$ Å for r_2 and r_4 , relative to the C–C bond distances in $\mathbf{1}^{1-}$). The fact that $\mathbf{1}^{1-}$ is observed while $\mathbf{1}^{2-}$ is not suggests that these changes could be key to promoting the cyclization cascade.

To further investigate the core annulation process, we calculated a hypothetical mono-annulated intermediate, $\mathbf{1_{mono}}^{2-}$ (Fig. 8b), in which only one site (the one corresponding to r_1) has undergone cyclization and dehydrogenation and is rearomatized. For this intermediate, the differences between the sites become even more pronounced: the site located *trans* to the cyclization has the shortest C–C distance ($r_3=3.007$ Å), which is substantially shorter than the C–C distances in the *gem* and *cis* sites ($r_2=3.129$ and $r_4=3.131$ Å, respectively). The significant shortening of the separation between the carbon atoms in the *trans* site is in line with the experimental evidence that the $\mathbf{1_{mono}}^{2-}$ intermediate is not observed. Therefore, it is entirely reasonable that this hypothetical intermediate could undergo spontaneous cyclization, and that it would be a regioselective process.

Hence, from a geometric perspective, we conclude that some geometric differences are introduced already in the neutral parent system, which subsequently create a preference for certain regioselectivity. The two helical sites that are *trans* to one another appear to be structurally aligned for cyclization more so than the counterpart pair (in contrast to our previous studies, where geometric differences were only introduced upon reduction).⁶⁷ Following the first annulation event, the site that is *trans* becomes even more primed than any of the other three sites and is likely to also cyclize spontaneously.

Frontier molecular orbitals

To provide further insights, we examined the frontier molecular orbitals of **1**, **1**¹⁻, and **1**²⁻. For the highest occupied molecular orbital (HOMO) of **1**, no constructive overlap was evident between any of the C-C pairs that could, in principle, form a new bond upon cyclization (Fig. S18†). In contrast, such an overlap did appear in the lowest unoccupied molecular orbital (LUMO), indicating that populating that orbital with electrons (*e.g.*, by chemical reduction) could promote the formation of a new C-C bond. Indeed, a similar overlap was observed in the singly-occupied molecular orbital (SOMO) of **1**¹⁻, in the HOMO of **1**²⁻, and in the HOMO of **1**_{mono}²⁻. As all three of these are (partially) filled orbitals, this implies the existence of a bonding interaction.

Despite the geometrical differences detailed above, the MO analysis could not provide further insight into the regioselectivity of the reaction. The visual differences in the MOs between the sites were too small to readily distinguish a preference for cyclization at one site over another. Similarly, the MOs for the hypothetical $\mathbf{1_{mono}}^{2-}$ did not indicate a substan-

tially better overlap at the *trans* site than at the other sites. Thus, the MO analysis is consistent with the nascent C–C bond alteration but does not allow us to rationalize the regioselectivity of the cyclization cascade.

Aromaticity

Finally, we turned to analysing the aromatic character of the twistacene series, covering four different reduced states and including the putative intermediates of the cyclization process, as well as the products of the cyclization and reduction reactions. In Fig. 9, we detail the nucleus-independent chemical shift (NICS)^{68–70} values for 1, 1^{1-} , 1^{2-} , 1_{mono}^{2-} , 1_{bis}^{2-} , and 1_{bis}^{4-} (the doubly-annulated dianion and tetraanion that were experimentally observed) using the NICS(1.7)_{ZZ} metric.⁷¹

We first studied the changes that occur following reduction of the polycyclic twistacene system. Upon reduction to 1¹⁻, the greatest changes are seen in the three middle rings of the pentacene core, which shift from markedly aromatic in 1 (Σ NICS $(1.7)_{ZZ} = -15$ and -20 ppm) to weakly aromatic in $\mathbf{1}^{1-}$ (Σ NICS $(1.7)_{ZZ} = -8$ and -5 ppm) to non-aromatic in $\mathbf{1}^{2-}$ ($\Sigma NICS(1.7)_{ZZ} =$ -1 and +4 ppm). In contrast, the pendant rings and the flanking rings at the edges of the pentacene core retain their respective $NICS(1.7)_{ZZ}$ values throughout and show very little change. These observations agree with the spin density location for 1^{1-} (see ESI, Fig. S20†) - the unpaired electron is localized on the middle three rings of the pentacene unit, thus it is unsurprising that only these rings exhibit changes to their aromatic character. Overall, the global molecular aromaticity, which was evaluated using the sum of $NICS(1.7)_{ZZ}$ values, sequentially decreases with the addition of negative charge $(\Sigma NICS(1.7)_{ZZ} = -179, -152, \text{ and}$ -127 ppm, for 1, 1^{1-} , and 1^{2-} , respectively). These results agree with other reported cases,⁶⁷ in which reduction of polycyclic

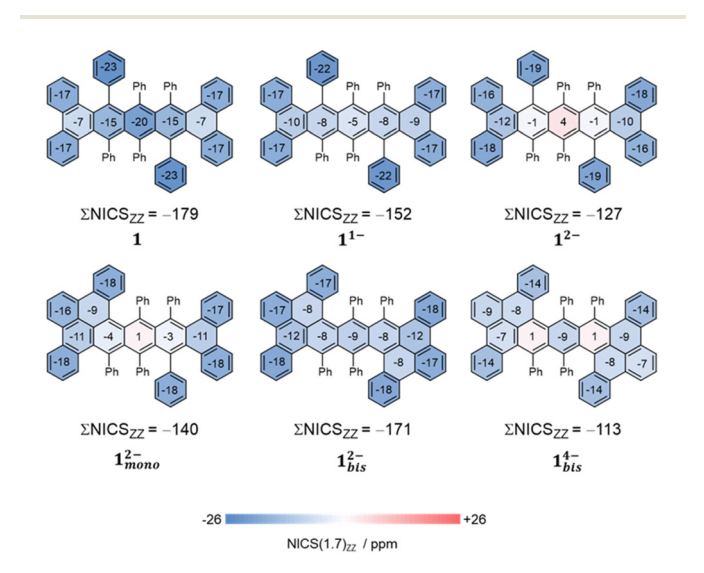


Fig. 9 NICS(1.7)_{ZZ} values for the investigated 1, 1^{1-} , 1^{2-} , 1_{mono}^{2-} , 1_{bis}^{2-} , and 1_{bis}^{4-} reported for each ring in ppm and rounded to the nearest integer. Ring-filled colors correspond to the color bar at the bottom: blue = diatropic (aromatic), red = paratropic (antiaromatic). Color intensity is proportional to the magnitude of the NICS(1.7)_{ZZ} value.

systems leads to loss of aromaticity and, in some cases, even gain of antiaromaticity.^{50,51}

Next, we studied the effects of cyclization, going from $\mathbf{1}^{2-}$ to $\mathbf{1_{mono}}^{2-}$ and finally to $\mathbf{1_{bis}}^{2-}$. Following the first cyclization, the global NICS value for $\mathbf{1_{mono}}^{2-}$ achieves $\Sigma \text{NICS}(1.7)_{ZZ} = -140$ ppm, which represents a gain of $\sim 10\%$ relative to the unmodified $\mathbf{1}^{2-}$. After the second cyclization, $\mathbf{1_{bis}}^{2-}$ has a $\Sigma \text{NICS}(1.7)_{ZZ} = -179$ ppm, which is comparable to $\mathbf{1}$, implying that the system has regained almost all of the aromaticity lost due to reduction. This may also explain the observation that $\mathbf{1}^{1-}$ is experimentally observed while $\mathbf{1}^{2-}$ is not – the latter is destabilized enough to spontaneously undergo core annulation.

Further addition of two more electrons to form the tetraanion again decreases the aromaticity, leading to $\Sigma NICS(1.7)_{ZZ} = -113$ ppm for $\mathbf{1_{bis}}^{4-}$. As opposed to the dianion, for the tetrareduced state, it is the second and fourth rings of the pentacene core that have the least negative NICS values. Despite the apparent loss of aromatic stabilization, there was no experimental evidence that $\mathbf{1_{bis}}^{4-}$ undergoes further cyclization at either of the remaining sites. This may be due to the geometrical constraints imposed by the pendant phenyl groups, as additional cyclization would lead to an increase in planarization that would force the pendant groups to be in closer proximity.

Metal complexation

With a better understanding of the "naked" twistacene in its different reduced states, we turned to studying π -complexation of the mono-, di-, and tetra-anionic species with either cesium or lithium cations. The total NICS(1.7)_{ZZ} values of product 2 (formed by 1^{1-} and Cs^{+} entrapped by two crown ethers), complex 3 (formed by 1_{bis}^{2-} and two $[Li^{+}(THF)_{2}]$ moieties) and complex 4 (formed by 1_{bis}^{4-} and two $[Li^{+}(THF)_{2}]$) are displayed in Fig. 10. We note that both anions are fully aromatic and, specifically, the values for the peripheral rings – those bearing hydrogens – are very similar to the neutral parent, 1. These results are in line with the experimental 1 H NMR data, which also show no significant uphill proton shift for the reduced products (Fig. S9 and S11†) compared to 1 (Fig. S6†).

As expected for a solvent separated-ion pair, the total charge of the polycyclic aromatic system in 2 is -0.97 and the total aromatic character is very similar to the uncomplexed 1^{1–} $(\Sigma NICS(1.7)_{ZZ} = -159 \text{ and } -151 \text{ ppm, respectively})$. This result agrees with the crystal structure of 2 showing no direct interaction between the metal ion and the monoanionic twistacene core, and hence the organic component retains its intrinsic properties. In contrast, the crystal structure of 3 is built on direct interactions between the 1_{bis}²⁻ core and two Li⁺ cations, and the consequences are clearly seen in the partial charge and aromaticity of the complexed aromatic ligand. There is a marked decrease in negative charge, to -1.45 (a loss of 27.5% of the charge, relative to 1^{2-}) and an increase in aromaticity to $\Sigma NICS(1.7)_{ZZ} = -204$ ppm (an increase of 19%, relative to -171 ppm for 1^{2-}). A similar change is seen for complex 4, in which the polycyclic aromatic component loses a substantial

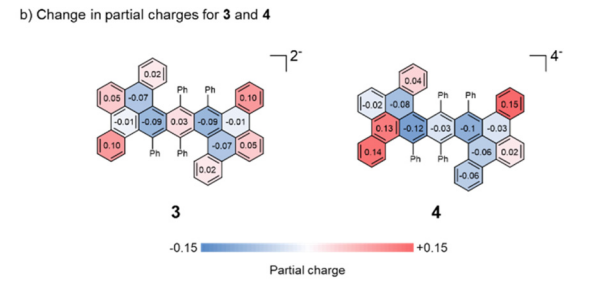


Fig. 10 NICS(1.7) $_{ZZ}$ values for the rings in the polycyclic aromatic moieties in complexes 2, 3, and 4 (a); the change in partial charge per ring, calculated as the difference of the sum of Löwdin charges of the carbons in each ring between the complexed and uncomplexed anionic moieties in 3 and 4 (b).

portion of its negative charge (changing from -4 to -3.22, a decrease of 20%), concomitant with an increase in aromaticity to $\Sigma NICS(1.7)_{ZZ} = -131$ ppm (16% increase, relative to $\mathbf{1}_{bis}^{4-}$).

To illustrate the changes incurred at a more local level, the partial charges on the carbon atoms comprising each ring were summed up. Upon complexation in 3, the penultimate pentacene ring and the newly formed ring of $\mathbf{1_{bis}}^{2-}$ display increased negative charges while all other rings decrease in partial charge (Fig. 10b shows the change in partial charge per ring). Similarly, in 4, the penultimate pentacene rings show the greatest increase in negative charge. In simple terms, the Li⁺-complexation causes a migration of charge density from the peripheral rings to the rings that are engaged in complexation, where the charge can be better stabilized through electrostatic cation-π interactions. The unique geometric features of complex 4 demonstrate this nicely, as the two Li⁺ ions are not complexed symmetrically with respect to the center of the tetraanion, and indeed it is the rings involved in Li⁺ ion binding that show the greatest increase in negative charge. Notably, this behaviour was also seen for the previously studied systems.67

Conclusions

In summary, the stepwise addition of multiple electrons to a twistacene was successfully accomplished using lithium and cesium metals to afford three new products covering three different reduction states. The products were crystallographically characterized to reveal only minor twistacene core changes upon one-electron addition followed a dramatic regioselective double-annulation caused by acquisition of the second electron. Interestingly, the injection of two more electrons did not result in any additional annulation processes.

We computationally investigated the source of regioselectivity and found that even though there are, in principle, four cyclization sites and three potential regioisomers that can be formed, the trans-situated sites are most likely to cyclize. These results agree with the observation that only the transtype bis-cyclized product is observed. Our computational analysis also revealed that double-reduction of the twistacene leads to a substantial decrease of aromaticity, most of which is regained in the cyclization and subsequent dehydrogenation steps. Indeed, the cyclization cascade stops after the second annulation, despite the system's charge and the existence of two remaining uncyclized sites. We believe this is due to the combination of aromatic stabilization of the bis-annulated product and the steric factors hindering further planarization. Therefore, although further reduction to the tetraanion results in loss of aromaticity, which may make additional cyclization more likely, the geometry of the carbon framework makes this less feasible.

In addition, the computational analysis allowed us to probe the changes incurred in the non-planar aromatic frameworks upon alkali metal ion complexation. Complexation helps to stabilize the structures through transfer of charge and concomitant increase of aromaticity. This is less successful in the Cs-product due to lack of direct metal ion- π interactions. The effects are more pronounced in the two π -complexes, in which two Li⁺ cations exhibit direct coordination to the respective carbanions. As a result, the aromatic moieties relieve a significant percentage of their negative charge (~25% and ~20%, respectively) and display an increase in their aromatic character (~20%).

As this work reports the first crystallographically characterized products of the reduced twistacene with alkali-metal counterions, it provides an exceptional foundation for comprehensive theoretical analysis of the consequence of stepwise electron addition to a twistacene core. As the stepwise reduction of twistacene 1 reveals a unique mechanism for expansion of the aromatic core through dehydrogenative annulation, this work could pave the way for ring closure reactions of other highly twisted polyarenes as an alternative to the Scholl reaction.

Author contributions

M. P. synthesized the reduced products, performed their characterization and structural description; Z. W. performed X-ray data collection and refinement; R. G. C. and K. V. K. synthesized parent twistacene; A. T. and R. G.-P. designed theoretical study, performed all calculations and data analysis; M. A. P. conceived and supervised this project; all authors participated in the result discussion and contributed to the manuscript preparation.

Conflicts of interest

There are no conflicts to declare.

Acknowledgements

Financial support of this work from the U. S. National Science Foundation, CHE-2003411 is gratefully acknowledged by M. A. P. NSF's ChemMatCARS, Sector 15 at the Advanced Photon Source (APS), Argonne National Laboratory (ANL) is supported by the Divisions of Chemistry (CHE) and Materials Research (DMR), National Science Foundation, under grant number NSF/CHE-1834750. This research used resources of the Advanced Photon Source, a U.S. Department of Energy (DOE) Office of Science user facility operated for the DOE Office of Science by Argonne National Laboratory under Contract No. DE-AC02-06CH11357. A. T. and R. G. P. acknowledge the financial and scientific support of Prof. Dr Peter Chen (ETH Zurich). R. G. P. is a Branco Weiss Fellow and a Horev Fellow. The authors also thank the anonymous reviewer for their helpful comments on symmetry analysis.

References

- 1 S. R. Peurifoy, T. J. Sisto, F. Ng, M. L. Steigerwald, R. Chen and C. Nuckolls, Dimensional control in contorted aromatic materials, *Chem. Rec.*, 2019, **19**, 1050–1061.
- 2 X. Qiao, D. M. Ho and R. A. Pascal Jr., An extraordinarily twisted polycyclic aromatic hydrocarbon, *Angew. Chem., Int. Ed. Engl.*, 1997, **36**, 1531–1532.
- 3 R. A. Pascal, Twisted acenes, *Chem. Rev.*, 2006, **106**, 4809–4819.
- 4 L. Palomo, F. G. Gámez, A. Bedi, O. Gidron, J. Casado and F. J. Ramírez, Raman and ROA analyses of twisted anthracenes: connecting vibrational and electronic/photonic structures, *Phys. Chem. Chem. Phys.*, 2021, 23, 13996–14003.
- 5 A. J.-T. Lou and T. J. Marks, A twist on nonlinear optics: Understanding the unique response of π -twisted chromophores, *Acc. Chem. Res.*, 2019, **52**, 1428–1438.
- 6 C. Zhan and J. Yao, More than conformational "twisting" or "coplanarity": Molecular strategies for designing high-efficiency nonfullerene organic solar cells, *Chem. Mater.*, 2016, 28, 1948–1964.
- 7 R. H. Barbour, A. A. Freer and D. D. MacNicol, The first synthesis of octakis(arylthio)naphthalenes: an X-ray study of a novel pressure-induced colour and conformational change in crystalline octakis(phenylthio)naphthalene, *J. Chem. Soc., Chem. Commun.*, 1983, 362–363.
- 8 J. D. Debad, S. K. Lee, X. Qiao, R. A. Pascal Jr. and A. J. Bard, Electrogenerated chemiluminescence 60. Spectroscopic properties and electrogenerated chemiluminescence of decaphenylanthracene and octaphenylnaphthalene, *Acta Chem. Scand.*, 1998, **52**, 45–50.

- 9 L. Tong, D. M. Ho, N. J. Vogelaar, C. E. Schutt and R. A. Pascal Jr., The albatrossenes: Large, cleft-containing, polyphenyl polycyclic aromatic hydrocarbons, *J. Am. Chem. Soc.*, 1997, **119**, 7291–7302.
- 10 J. Michl and E. C. H. Sykes, Molecular rotors and motors: Recent advances and future challenges, *ACS Nano*, 2009, 3, 1042–1048.
- 11 E. R. Kay, D. A. Leigh and F. Zerbetto, Synthetic molecular motors and mechanical machines, *Angew. Chem., Int. Ed.*, 2007, **46**, 72–191.
- 12 S. K. Mellerup and S. Wang, Boron-based stimuli responsive materials, *Chem. Soc. Rev.*, 2019, **48**, 3537–3549.
- 13 F. Tian, T. Wang, W. Dang, J. Xiao and X. Zhao, Efficient electroluminescence from twistacene-modified π-conjugated compounds, *Dyes Pigm.*, 2020, 177, 108298.
- 14 J. Xiao, Y. Divayana, Q. Zhang, H. M. Doung, H. Zhang, F. Boey, X. W. Sun and F. Wudl, Synthesis, structure, and optoelectronic properties of a new twistacene 1,2,3,4,6,13-hexaphenyl-7:8,11:12-bisbenzo-pentacene, *J. Mater. Chem.*, 2010, 20, 8167–8170.
- 15 M. A. Bryden and E. Zysman-Colman, Organic thermally activated delayed fluorescence (TADF) compounds used in photocatalysis, *Chem. Soc. Rev.*, 2021, **50**, 7587–7680.
- 16 X. Wei, Z. Liu, K. Zhang, Z. Zhao, W. Zhang, Q. Han, G. Ma and C. Zhang, "Hot exciton" fluorescence and charge transport of fine-tuned twistacenes: theoretical study on substitution effect and intermolecular interactions, *New J. Chem.*, 2023, 47, 3847–3855.
- 17 Y. Liu, C. Li, Z. Ren, S. Yan and M. R. Bryce, All-organic thermally activated delayed fluorescence materials for organic light-emitting diodes, *Nat. Rev. Mater.*, 2018, 3, 1–20.
- 18 G. Song, X. Wu, W. Zhou, J. Xiao, X. Zhang, Y. Wang and Y. Song, Pulse-width-dependent optical limiting properties of a novel twist-acene compound, *Opt. Mater.*, 2023, **136**, 113394.
- 19 W. Wang, Z. Yuan, S. Wang, X. Li, B. Ji and J. Xiao, Effect of annulation mode of twistarene on the physical property and self-assembly behavior of functionalized curved aromatic molecules, *Chem. Eur. J.*, 2022, **28**, e202201233.
- 20 T. Ren, M. Song, J. Zhao, W. Wang, X. Shen, C. Gao, Y. Yi and J. Xiao, Twistacene functionalized anthracenes with high-efficiency blue fluorescence, *Dyes Pigm.*, 2016, 125, 356–361.
- 21 R. Benshafrut, E. Shabtai, M. Rabinovitz and L. T. Scott, π -Conjugated anions: From carbon-rich anions to charged carbon allotropes, *Eur. J. Org. Chem.*, 2000, 1091–1106.
- 22 M. D. Tzirakis and M. Orfanopoulos, Radical reactions of fullerenes: From synthetic organic chemistry to materials science and biology, *Chem. Rev.*, 2013, **113**, 5262–5321.
- 23 D. Eisenberg and R. Shenhar, Polyarene anions: interplay between theory and experiment, *Wiley Interdiscip. Rev.: Comput. Mol. Sci.*, 2012, 2, 525–547.
- 24 A. V. Zabula and M. A. Petrukhina, Structural perspective on aggregation of alkali metal ions with charged planar and curved carbon π -surfaces, in *Adv. Organomet. Chem*, ed.

- A. F. Hill and M. J. Fink, Academic Press, 2013, vol. 61, pp. 375–462.
- 25 M. M. Haley and R. R. Tykwinski, *Carbon-rich compounds: From molecules to materials*, John Wiley & Sons, 2006.
- 26 A. V. Zabula, S. N. Spisak, A. S. Filatov, V. M. Grigoryants and M. A. Petrukhina, How charging corannulene with one and two electrons affects its geometry and aggregation with sodium and potassium cations, *Chem. Eur. J.*, 2012, **18**, 6476–6484.
- 27 S. N. Spisak, Z. Wei, E. Darzi, R. Jasti and M. A. Petrukhina, Highly strained [6]cycloparaphenylene: crystallization of an unsolvated polymorph and the first mono- and dianions, *Chem. Commun.*, 2018, 54, 7818–7821.
- 28 S. N. Spisak, M. U. Bühringer, Z. Wei, Z. Zhou, R. R. Tykwinski and M. A. Petrukhina, Structural and electronic effects of stepwise reduction of a tetraaryl[3]cumulene, *Angew. Chem.*, 2019, 131, 2045–2050.
- 29 Y. Zhu, Z. Zhou, Z. Wei and M. A. Petrukhina, Two-fold reduction of dibenzo[a,e]cyclooctatetraene with group 1 metals: From lithium to cesium, *Organometallics*, 2020, **39**, 4688–4695.
- 30 A. V. Zabula, A. S. Filatov, J. Xia, R. Jasti and M. A. Petrukhina, Tightening of the nanobelt upon multi-electron reduction, *Angew. Chem., Int. Ed.*, 2013, **52**, 5033–5036.
- 31 D. Eisenberg, E. A. Jackson, J. M. Quimby, L. T. Scott and R. Shenhar, The bicorannulenyl dianion: A charged overcrowded ethylene, *Angew. Chem.*, 2010, **122**, 7700–7704.
- 32 A. Ayalon, A. Sygula, P.-C. Cheng, M. Rabinovitz, P. W. Rabideau and L. T. Scott, Stable high-order molecular sandwiches: Hydrocarbon polyanion pairs with multiple lithium ions inside and out, *Science*, 1994, 265, 1065–1067.
- 33 H. Bock, K. Gharagozloo-Hubmann, M. Sievert, T. Prisner and Z. Havlas, Single crystals of an ionic anthracene aggregate with a triplet ground state, *Nature*, 2000, **404**, 267–269.
- 34 A. V. Zabula, S. N. Spisak, A. S. Filatov, A. Yu. Rogachev and M. A. Petrukhina, Record alkali metal intercalation by highly charged corannulene, *Acc. Chem. Res.*, 2018, 51, 1541–1549.
- 35 Z. Zhou, S. N. Spisak, Q. Xu, A. Yu. Rogachev, Z. Wei, M. Marcaccio and M. A. Petrukhina, Fusing a planar group to a π-bowl: Electronic and molecular structure, aromaticity and solid-state packing of naphthocorannulene and its anions, *Chem. Eur. J.*, 2018, **24**, 3455–3463.
- 36 S. N. Spisak, Z. Wei, N. J. O'Neil, A. Yu. Rogachev, T. Amaya, T. Hirao and M. A. Petrukhina, Convex and concave encapsulation of multiple potassium ions by sumanenyl anions, *J. Am. Chem. Soc.*, 2015, 137, 9768– 9771.
- 37 T. Wombacher, R. Goddard, C. W. Lehmann and J. J. Schneider, Complete charge separation provoked by full cation encapsulation in the radical mono- and dianions of 5,6:11,12-di-o-phenylene-tetracene, *Dalton Trans.*, 2018, 47, 10874–10883.
- 38 Y. Zhang, Y. Zhu, D. Lan, S. H. Pun, Z. Zhou, Z. Wei, Y. Wang, H. K. Lee, C. Lin, J. Wang, M. A. Petrukhina, Q. Li

- and Q. Miao, Charging a negatively curved nanographene and its covalent network, *J. Am. Chem. Soc.*, 2021, **143**, 5231–5238.
- 39 N. Treitel, T. Sheradsky, L. Peng, L. T. Scott and M. Rabinovitz, C₃₀H₁₂⁶⁻: Self-aggregation, high charge density, and pyramidalization in a supramolecular structure of a supercharged hemifullerene, *Angew. Chem.*, 2006, 118, 3351–3355.
- 40 A. V. Zabula, A. S. Filatov, S. N. Spisak, A. Yu. Rogachev and M. A. Petrukhina, A main group metal sandwich: Five lithium cations jammed between two corannulene tetraanion decks, *Science*, 2011, 333, 1008–1011.
- 41 T. Wombacher, R. Goddard, C. W. Lehmann and J. J. Schneider, Bowl shaped deformation in a planar aromatic polycycle upon reduction. Li and Na separated dianions of the aromatic polycycle 5,6:11,12-di-o-phenylenetetracene, *Dalton Trans.*, 2017, 46, 14122–14129.
- 42 H. Bock, Z. Havlas, K. Gharagozloo-Hubmann and M. Sievert, The Li⁺-initiated twofold dehydrogenation and C–C bond formation of hexaphenylbenzene to the dilithium salt of the 9,10-diphenyltetrabenz[a,c,h,j]anthracene dianion, *Angew. Chem., Int. Ed.*, 1999, 38, 2240–2243.
- 43 Z. Zhou, Y. Zhu, Z. Wei, J. Bergner, C. Neiß, S. Doloczki, A. Görling, M. Kivala and M. A. Petrukhina, Reversible structural rearrangement of π-expanded cyclooctatetraene upon two-fold reduction with alkali metals, *Chem. Commun.*, 2022, 58, 3206–3209.
- 44 S. N. Spisak, A. V. Zabula, M. Alkan, A. S. Filatov, A. Yu. Rogachev and M. A. Petrukhina, Site-directed dimerization of bowl-shaped radical anions to form a σ-bonded dibenzocorannulene dimer, *Angew. Chem., Int. Ed.*, 2018, 57, 6171–6175.
- 45 I. Aprahamian, D. V. Preda, M. Bancu, A. P. Belanger, T. Sheradsky, L. T. Scott and M. Rabinovitz, Reduction of bowl-shaped hydrocarbons: Dianions and tetraanions of annelated corannulenes, *J. Org. Chem.*, 2006, 71, 290–298.
- 46 A. Yu. Rogachev, M. Alkan, J. Li, S. Liu, S. N. Spisak, A. S. Filatov and M. A. Petrukhina, Mono-reduced corannulene: To couple and not to couple in one crystal, *Chem. Eur. J.*, 2019, 25, 14140–14147.
- 47 I. Aprahamian, R. E. Hoffman, T. Sheradsky, D. V. Preda, M. Bancu, L. T. Scott and M. Rabinovitz, A four-step alternating reductive dimerization/bond cleavage of indenocorannulene, *Angew. Chem., Int. Ed.*, 2002, 41, 1712–1715.
- 48 M. Rickhaus, A. P. Belanger, H. A. Wegner and L. T. Scott, An oxidation induced by potassium metal. Studies on the anionic cyclodehydrogenation of 1,1'-binaphthyl to perylene, *J. Org. Chem.*, 2010, 75, 7358–7364.
- 49 A. Ayalon and M. Rabinovitz, Reductive ring closure of helicenes, *Tetrahedron Lett.*, 1992, **33**, 2395–2398.
- 50 Z. Zhou, R. K. Kawade, Z. Wei, F. Kuriakose, Ö. Üngör, M. Jo, M. Shatruk, R. Gershoni-Poranne, M. A. Petrukhina and I. V. Alabugin, Negative charge as a lens for concentrating antiaromaticity: Using a pentagonal "defect" and helicene strain for cyclizations, *Angew. Chem., Int. Ed.*, 2020, 59, 1256–1262.

- 51 Z. Zhou, D. T. Egger, C. Hu, M. Pennachio, Z. Wei, R. K. Kawade, Ö. Üngör, R. Gershoni-Poranne, M. A. Petrukhina and I. V. Alabugin, Localized antiaromaticity hotspot drives reductive dehydrogenative cyclizations in bis- and mono-helicenes, *J. Am. Chem. Soc.*, 2022, 144, 12321–12338.
- 52 R. G. Clevenger, B. Kumar, E. M. Menuey and K. V. Kilway, Synthesis and structure of a longitudinally twisted hexacene, *Chem. Eur. J.*, 2018, **24**, 3113–3116.
- 53 P. Jin, T. Song, J. Xiao and Q. Zhang, Recent progress in using pyrene-4,5-diketones and pyrene-4,5,9,10-tetraketones as building blocks to construct large acenes and heteroacenes, *Asian J. Org. Chem.*, 2018, 7, 2130–2146.
- 54 X. Deng, X. Liu, L. Wei, T. Ye, X. Yu, C. Zhang and J. Xiao, Pentagon-containing π -expanded systems: Synthesis and photophysical properties, *J. Org. Chem.*, 2021, **86**, 9961–9969.
- 55 C. Wei, J. Wu, D. Zhang, W. Su, J. Xiao and Z. Cui, Molecular modulation based on the terminal substituent in twistacenes for organic light-emitting diodes, *Asian J. Org. Chem.*, 2018, 7, 424–431.
- 56 T. J. Sisto, Y. Zhong, B. Zhang, M. T. Trinh, K. Miyata, X. Zhong, X.-Y. Zhu, M. L. Steigerwald, F. Ng and C. Nuckolls, Long, atomically precise donor-acceptor coveedge nanoribbons as electron acceptors, *J. Am. Chem. Soc.*, 2017, 139, 5648–5651.
- 57 X. Li, L. Wei, F. Tian, X. Deng, X. Zhao and J. Xiao, Expanded benzofuran-decorated twistacene derivatives: synthesis, characterization and single-component white electroluminescence, *Phys. Chem. Chem. Phys.*, 2020, 22, 12166–12172.
- 58 H. M. Duong, M. Bendikov, D. Steiger, Q. Zhang, G. Sonmez, J. Yamada and F. Wudl, Efficient synthesis of a novel, twisted and stable, electroluminescent "twistacene", *Org. Lett.*, 2003, 5, 4433–4436.
- 59 Y. Han, J. Xiao, X. Wu, Y. Wang, X. Zhang and Y. Song, Doubly 1,3-butadiyne-bridged ditwistacene with enhanced ultrafast broadband reverse saturable absorption, *J. Mater. Chem. C*, 2022, **10**, 14122–14127.
- 60 H. M. Bergman, D. D. Beattie, G. R. Kiel, R. C. Handford, Y. Liu and T. D. Tilley, A sequential cyclization/π-extension strategy for modular construction of nanographenes enabled by stannole cycloadditions, *Chem. Sci.*, 2022, **13**, 5568–5573.
- 61 W. Fan, T. Winands, N. L. Doltsinis, Y. Li and Z. Wang, A decatwistacene with an overall 170° torsion, *Angew. Chem., Int. Ed.*, 2017, **56**, 15373–15377.
- 62 F. Tian, T. Song, T. Wang, J. Xiao and X. Zhao, 11,16-Ditert-butyl-9,18-diphenylbenzo[kl]benzo[8,9]triphenyleno [2,3-b]xanthene: Synthesis, photophysics, self-assembly and electroluminescent properties, *Asian J. Org. Chem.*, 2019, **8**, 399–403.
- 63 R. G. Clevenger, F. Kumar, E. M. Menuey, G.-H. Lee, D. Patterson and K. V. Kilway, A superior synthesis of longitudinally twisted acenes, *Chem. – Eur. J.*, 2018, 24, 243–250.

- 64 Z. Zhou, Z. Wei, Y. Tokimaru, S. Ito, K. Nozaki and M. A. Petrukhina, Stepwise reduction of azapentabenzocorannulene, Angew. Chem., Int. Ed., 2019, 58, 12107-12111.
- 65 J. Lu, D. M. Ho, N. J. Vogelaar, C. M. Kraml, S. Bernhard, N. Byrne, L. R. Kim and R. A. Pascal Jr., Synthesis, structure, and resolution of exceptionally twisted pentacenes, J. Am. Chem. Soc., 2006, 128, 17043-17050.
- 66 J. Lu, D. M. Ho, N. J. Vogelaar, C. M. Kraml and R. A. Pascal Jr., A pentacene with a 144° twist, J. Am. Chem. Soc., 2004, 126, 11168-11169.
- 67 Z. Zhou, Ö. Üngör, Z. Wei, M. Shatruk, A. Tsybizova, R. Gershoni-Poranne and M. A. Petrukhina, Tuning magnetic interactions between triphenylene radicals by variation of crystal packing in structures with alkali metal counterions, Inorg. Chem., 2021, 60, 14844-14853.
- 68 P. v. R. Schleyer, C. Maerker, A. Dransfeld, H. Jiao and N. J. R. van Eikema Hommes, Nucleus-independent chemical shifts: A simple and efficient aromaticity probe, J. Am. Chem. Soc., 1996, 118, 6317-6318.
- 69 Z. Chen, C. S. Wannere, C. Corminboeuf, R. Puchta and P. v. R. Schlever, Nucleus-independent chemical shifts (NICS) as an aromaticity criterion, Chem. Rev., 2005, 105, 3842-3888.
- 70 R. Gershoni-Poranne and A. Stanger, NICS-nucleus independent chemical shift, in Aromaticity, ed. I. Fernandez, Elsevier, 2021, pp. 99-154.
- 71 R. Gershoni-Poranne and A. Stanger, The NICS-XYscan: Identification of local and global ring currents in multi-ring systems, Chem. - Eur. J., 2014, 20, 5673-